The interoceptive self contributes to preference stability

Azzalini D.*, Buot A., Palminteri S. & Tallon-Baudry C.*

Laboratoire de Neurosciences Cognitives et Computationnelles, Ecole Normale Supérieure, PSL University & Institut National de la Santé et de la Recherche Médicale, 75005, Paris, France

* Corresponding authors: damiano.azzalini@gmail.com, catherine.tallon-baudry@ens.psl.eu.

Abstract

Forrest Gump or Matrix? Choosing which movie you prefer is a subjective decision that entails self-reflection. While the neural underpinnings of valuation and choice have been extensively investigated, the contribution of self-related processes to subjective decisions has been largely overlooked. Self-related processes have been linked to a basic interoceptive biological mechanism, the neural monitoring of heartbeats, in particular in ventromedial prefrontal cortex (vmPFC), a region also involved in value encoding. We thus hypothesized a functional coupling between interoceptive self-related processes and the precision of value encoding in vmPFC. Human participants were presented with pairs of movie titles. They indicated either which movie they preferred, or performed a control objective visual discrimination that did not require self-reflection. Using magnetoencephalography, we measured heartbeat-evoked responses (HERs) before option presentation, and confirmed that HERs in vmPFC were larger when preparing to the subjective, self-related task. We retrieved the expected cortical value network during choice with time-resolved statistical modeling, and show that HERs before option presentation interacted in a multiplicative manner with value encoding during choice in vmPFC. The interaction was absent in the objective discrimination task, and could not be trivially explained neither by changes in cardiac activity nor by arousal fluctuations. The neural interaction between HERs and value encoding predicted preference-based choice consistency over time, accounting for both inter-individual differences and trial-to-trial fluctuations within individuals. Our results thus reveal a functional coupling in vmPFC between self-related interoceptive processes and subjective value encoding, which stabilizes the behavioral expression of long-term preferences.

Keywords

Interoception, self, brain-body interaction, preferences, MEG.

45 **Significance statement**

46 Deciding whether you prefer Forrest Gump or Matrix is based on subjective values, which only
47 you, the decision-maker, can estimate and compare, by asking yourself. Yet, how self-related processes
48 influence subjective valuation is not known. We show that in ventromedial prefrontal cortex, an
49 interoceptive self-related process, the neural response to heartbeats, influences the cortical
50 representation of subjective value. The neural interaction between interoceptive self-related process and
51 value encoding predicts choice consistency, i.e. whether you consistently prefer Forrest Gump over
52 Matrix over time, thus contributing to the stable expression of long-lasting preferences that define, at
53 least in part, our identity.

54

Introduction

Do you prefer Forrest Gump or Matrix? The decision is subjective: only *you* know which movie you like best. The subjective values used in preference-based decision making are internally generated, intrinsically private, and entail self-reflection. In other words, estimating a subjective value requires a reflection about how an item affects *you*. In contrast, the evidence required to decide which of the two words 'listen' and 'look' has more characters is publicly and objectively available to any reader of this article. While the neural underpinnings of valuation and choice have been well studied, the biological mechanism supporting the self-reflection intrinsic to subjective decisions remains unspecified. It might derive from the simplest biological implementation of self-reflection, i.e., the monitoring of one's current physiological state (1–5) required to select the most appropriate behavior to restore homeostatic balance thus ensuring the integrity of the living organism. It follows that the organism needs to track its internal state to assign a value to a given option (6, 7), and that a corruption of the representation of the internal state may lead to suboptimal choice (8). Such interoceptive self-related processes might also underlie subjective choices that have no immediate physiological consequences.

The monitoring of current physiological state is notably indexed by the transient neural response automatically elicited by each heartbeat, also known as the heartbeat-evoked response (HER)(9, 10). HERs have been linked to subjective, self-related cognitive processes in ventromedial prefrontal cortex (vmPFC)(11–13). A separate stream of studies repeatedly showed that vmPFC encodes subjective values (14–16). We thus hypothesized that (a) HERs in vmPFC would signal the interoceptive self-related processes recruited when preparing to a subjective decision, but absent when preparing to an objective decision and (b) that HER fluctuations would affect valuation in subjective preference-based decisions, but not in decisions based on objective evidence publicly available in the outside world, such as perceptual discriminations. We tested these hypotheses in a paradigm where participants performed either a subjective, preference-based choice, or a control, objective perceptual discrimination, between two visually presented movie titles (**Fig. 1**), while their neural and cardiac activity were measured with magnetoencephalography (MEG) and electrocardiography (ECG),

respectively. Each trial began with an instruction period, with a symbol indicating which type of decision to perform, during which we measured HERs. Once options were displayed, participants selected the title of the movie they preferred in subjective preference trials, and the title written with the highest contrast in objective perceptual discrimination trials. We found that (a) HERs during the instruction period were larger when preparing for preference-based decisions than for discrimination ones, and we demonstrated that (b) HER amplitude interacted with the neural encoding of subjective value in vmPFC during choice. The neural interaction between HER and value encoding was associated with more consistent subjective choices. Those effects were absent in objective visual discrimination trials.

Results

Behavioral results

Participants were asked to choose between two simultaneously presented movie titles according either to their subjective preferences or to the visual contrast of movie titles, as indicated by trial-by-trial instructions presented before the alternatives (**Fig. 1A**). Decision difficulty, operationalized as the difference between the two options (difference between likeability ratings measured one day before the MEG session in the preference task (**Supplementary Fig.1**), difference between contrasts in the perceptual task), had the expected impact on behavior in both tasks. Both preference consistency and discrimination accuracy increased and reaction times decreased for easier decisions (**Fig. 1C**; preference task, one-way repeated measure ANOVA, main effect of difficulty: accuracy, $F_{(3,60)} = 99.25$, $p < 10^{-15}$; RT, $F_{(3,60)} = 41.14$, $p < 10^{-13}$; perceptual task, main effect of difficulty: accuracy, $F_{(3,60)} = 280.2$, $p < 10^{-15}$; RT, $F_{(3,60)} = 87.67$, $p < 10^{-15}$). Preference and perceptual decisions were matched in accuracy (two-way repeated measures ANOVA, main effect of task on accuracy, $F_{(1,20)} = 0.38$, $p = 0.55$, interaction task x difficulty, $F_{(3,60)} = 2.53$, $p = 0.07$), but preference-based decisions were generally slower (two-way repeated measures ANOVA, main effect of task, RT, $F_{(1,20)} = 57.64$, $p < 10^{-6}$) and reaction times decreased less rapidly for easier decisions (interaction task x difficulty, $F_{(3,60)} = 4.08$, $p = 0.01$). Participants only used task-relevant information (subjective value or objective contrast) to decide, since non-relevant information could not predict choice (**Fig. 1D**; **Supplementary Table 1**).

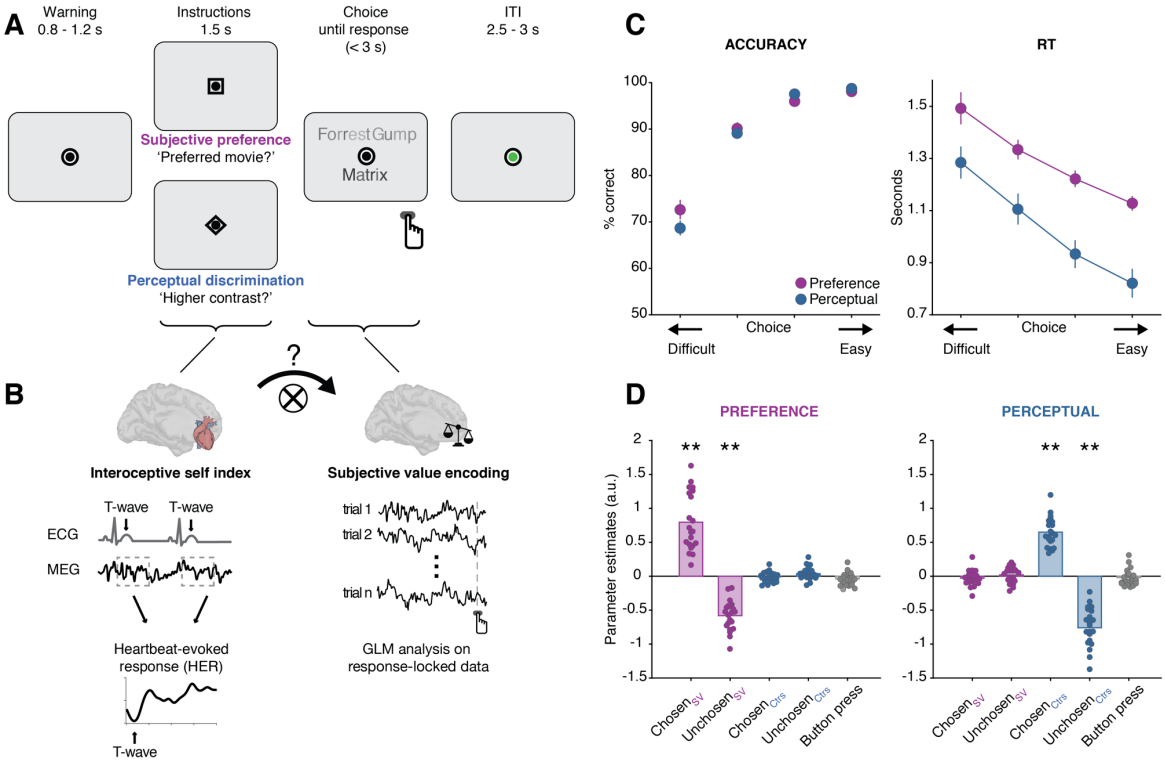

Fig. 1. Experimental design and behavioral results. **A**, Trial time-course. After a fixation period of variable duration, a symbol (square or diamond) instructed participants on the type of decision to perform on the upcoming movie titles, either a subjective preference-based choice or an objective perceptual discrimination task. Decision type varied on a trial-by-trial basis. The two movie titles appeared above and below fixation and remained on screen until response or until 3 seconds had elapsed. **B**, Rationale for data analysis. Left, interoceptive self processes were indexed by heartbeat-evoked responses (HERs) computed during the instruction period, before option presentation, by averaging MEG activity locked to the T-waves of the electrocardiogram. Right, response-locked MEG activity during choice was modeled on a trial-by-trial basis with a GLM to isolate the spatio-temporal patterns of neural activity encoding value. The central question is whether HERs before option presentation and value encoding interact. **C**, Behavioral results. In both tasks, performance (choice consistency or discrimination accuracy) increased ($F(3,60) = 99.25$, $p < 10^{-15}$) and response times decreased ($F(3,60) = 41.14$, $p < 10^{-13}$) for easier choices (i.e. larger difference in subjective value for preference-based decisions, or difference in contrast for perceptual ones). **D**, Only task-relevant information significantly contributed to choice in both preference-based and perceptual decisions as

estimated by logistic regression (two-tailed t-test against zero). Each dot represents one participant. **$p<0.01$.

129 **Neural responses to heartbeats are larger when preparing for preference-based decisions**

130 HERs in vmPFC have been previously shown to index self-related processes (11–13). We thus
131 predicted that HERs would be larger when preparing for subjective, preference-based decisions relying
132 on self-reflection than when preparing for objective, perceptual ones. Using a non-parametric clustering
133 procedure which corrects for multiple comparisons across time and space (17), we found that HERs
134 during the instruction period, before option presentation, were indeed larger when participants prepared
135 for preference-based decisions than for perceptual ones (**Fig. 2A**, **2B**; non-parametric clustering, 201-
136 262 ms after T-wave, sum(t) = 1789, Monte Carlo cluster level p = 0.037). Averaging cluster activity
137 separately in the two conditions results in an effect size Cohen's d of 1.28. The cortical regions that
138 mostly contributed to this effect (**Fig. 2C**, **Table 1**) were localized as expected in right and left anterior
139 vmPFC (areas 11m and 14 bilaterally; cluster peak at MNI coordinates, [1 57 -21] and [-3 47 -6]), but
140 also in the right post-central complex ([32 -22 56]) and right supramarginal gyrus ([41 -33 43]).

141

142 The HER difference between subjective preference-based trials and objective perceptual
143 discrimination trials was not accompanied by any difference in ECG activity (**Supplementary Table**
144 **2**), in cardiac parameters (inter-beat intervals, inter-beat intervals variability, stroke volume) or arousal
145 indices (alpha power and pupil diameter) measured during the instruction period (**Supplementary**
146 **Table 3**). The HER difference is thus neither due differences in cardiac inputs nor to overall changes
147 in brain state. Importantly, the HER difference was time-locked to heartbeats and thus did not reflect a
148 baseline difference between conditions (Monte-Carlo p=0.026. see **Methods** for details).

149

150 **The subjective value of the chosen option is encoded in medial prefrontal cortices in preference-**
151 **based decisions**

152 We then identified when and where subjective value was encoded during preference-based
153 choice. First, we modeled single trial response-locked neural activity at the sensor level using a GLM
154 (GLM1a, see **Methods**), using as regressors the subjective values of the chosen ($Chosen_{SV}$) and
155 unchosen ($Unchosen_{SV}$) options, as well as the response button used. Neural activity over frontal sensors

encoded the subjective value of the chosen option in two neighboring time-windows ($ß_{ChosenSV}$, first cluster: -580 to -370 ms before response, sum(t)=-7613, Monte Carlo p = 0.004. Second cluster: -336 to -197 ms before response, sum(t) = -4405, Monte Carlo p= 0.033; **Fig. 2D** and **Fig. 2E**). No cluster of neural activity significantly encoded the subjective value of the unchosen option. Motor preparation was encoded later in time in two posterior-parietal clusters of opposite polarities ($ß_{Button\ Press}$, negative cluster: -287 to -28 ms before response, sum(t) = -10918, Monte Carlo p = 0.003; positive cluster: -373 to -196 ms before response, sum(t) = 5848, Monte Carlo p = 0.02).

To identify the cortical regions contributing to the encoding of subjective value at sensor-level, we used the same model (GLM1a) to predict source-reconstructed activity averaged in the time-window identified at sensor level (-580 to -197 ms before response). The subjective value of the chosen option was encoded as expected in medial prefrontal regions (right posterior vmPFC area 32 and 24, cluster peak at MNI coordinates: [7 40 0]); right dorso-medial prefrontal cortex dmPFC area 8m [5 30 40]), as well as in bilateral occipital poles ([6 -77 11], [-1 -85 16]) and mid-posterior left insula ([-34 -27 17]) (**Fig. 2F**; **Supplementary Table 4**).

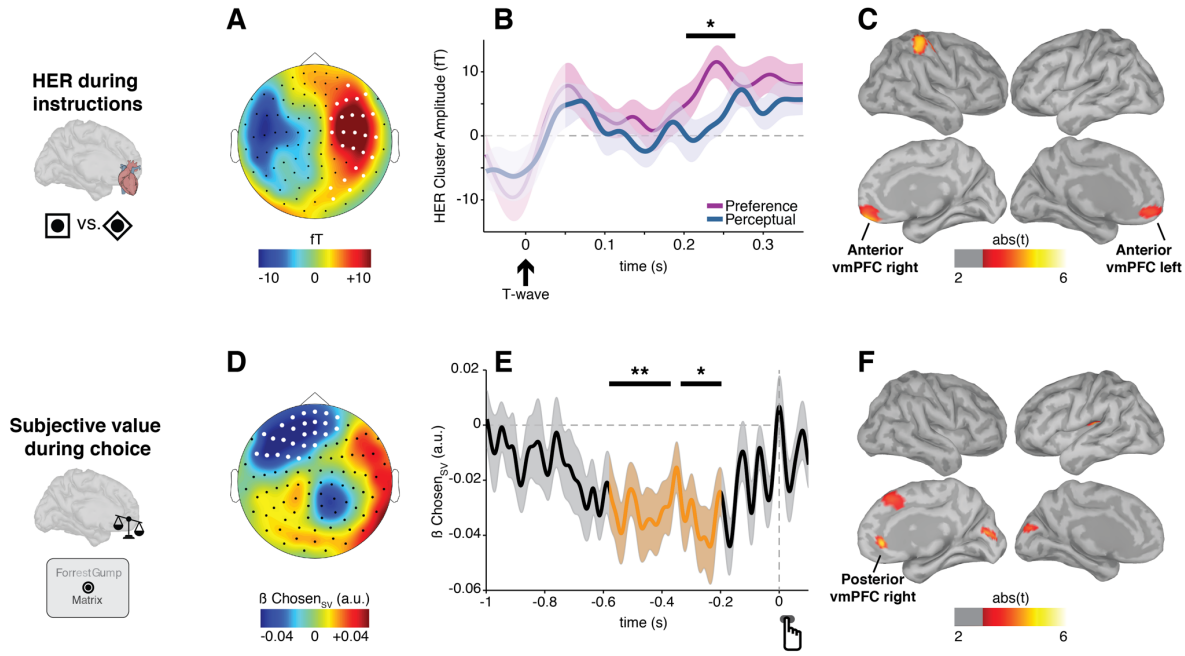

Fig. 2. **HERs and subjective value encoding. A**, Topography of the significant HER difference between preference-based and perceptual decisions during the instruction period (201-262 ms after cardiac T-wave, cluster Monte Carlo p = 0.037). **B**, Time-course of HER (± SEM) for preference-based and perceptual decisions in the cluster highlighted in white in A. The portion of the signal (50 ms after T-wave) still potentially contaminated by the cardiac artifact appears in lighter color. The black bar indicates the significant time-window, as established by non-parametric clustering procedure. **C**, Brain regions mostly contributing to the HER difference between preference-based and perceptual decisions (at least 20 contiguous vertices with uncorrected $p < 0.005$). **D,** Topography of the significant encoding of the chosen option subjective value (-580 to -197 ms before motor response) during choice in preference-based trials. **E**, Time-course (± SEM) of the GLM parameter estimate for the chosen option subjective value in the cluster highlighted in white in D. Black bars indicate significant time-windows, as established by non-parametric clustering procedure. **F**, Brain regions mostly contributing to the encoding of the subjective value of the chosen option (at least 20 contiguous vertices with uncorrected $p < 0.005$). *p<0.05, **p<0.01.

185 **Table 1. HER difference between preference-based and perceptual decisions. MNI coordinates**
186 **correspond to the voxel with maximal t-value.**
187

Peak *t* AAL atlas label	Peak *t* MNI coordinates (mm)	*t*-value
R Gyrus Rectus	[1 57 -21]	4.68
L medial orbitofrontal	[-3 47 -6]	3.76
R Post central complex	[32 -22 56]	5.57
R supramarginal gyrus	[41 -33 43]	3.98

188 **HER amplitude during instruction interacts with subjective value encoding in right vmPFC**
189 **during choice on a trial-by-trial basis**

190 We thus show that two different sub-regions of vmPFC were involved at different moments in
191 a trial: during the instruction period, HERs were larger when participants prepared for preference-based
192 vs. perceptual decisions in left and right anterior vmPFC, and during the choice period, subjective value
193 was encoded in right posterior vmPFC. We then addressed our main question (**Fig. 1B**): does the
194 amplitude of neural responses to heartbeats during the instruction period interact with the encoding of
195 subjective value during choice in vmPFC?

196 We tested whether subjective value encoding in right posterior vmPFC was affected by HER
197 amplitude measured in either left or right anterior vmPFC in a two-by-two ANOVA with HER
198 amplitude (high or low, median split across trials) and hemisphere as factors. The ANOVA revealed a
199 significant interaction between HER amplitude and hemisphere (**Fig. 3A**; $F_{(1,40)}$=5.07, p=0.036; no
200 main effect of HER amplitude $F_{(1,20)}$=2.69, p=0.12, no main effect of hemisphere $F_{(1,20)}$=0.19, p=0.67).
201 This interaction corresponded to a significantly stronger subjective value encoding in trials where
202 HERs in right vmPFC were larger during instructions (two-tailed paired t-test on $ß_{ChosenSV}$ in large vs.
203 small HER values in right vmPFC, $t_{(20)}$ = 2.52, p = 0.02, Cohen's d = 0.55).

204 The influence of HER amplitude was specific to value encoding: the amplitude of visual
205 responses evoked by option presentation was unrelated to HER amplitude (**Supplementary Table 5**).
206 HER amplitude is thus not a mere index of cortical responsiveness, interacting with any other brain
207 response. HER amplitude in r-vmPFC did not vary with pupil diameter nor alpha power, neither during

instructions nor choice (**Supplementary Table 5**), indicating that HER fluctuations are not driven by an overall change in brain state. Last, to definitively rule out an influence of attention/arousal, we tested whether the strength of value encoding was modulated by fluctuations in alpha power or pupil diameter measured during instructions. We median-split trials based on either alpha power or pupil but found no difference in value encoding (alpha, paired t-test on $ß_{ChosenSV}$ $t_{(20)}$=0.19, p=0.85, BF=0.25; pupil, paired t-test $t_{(20)}$=-0.23, p=0.82, BF=0.24).

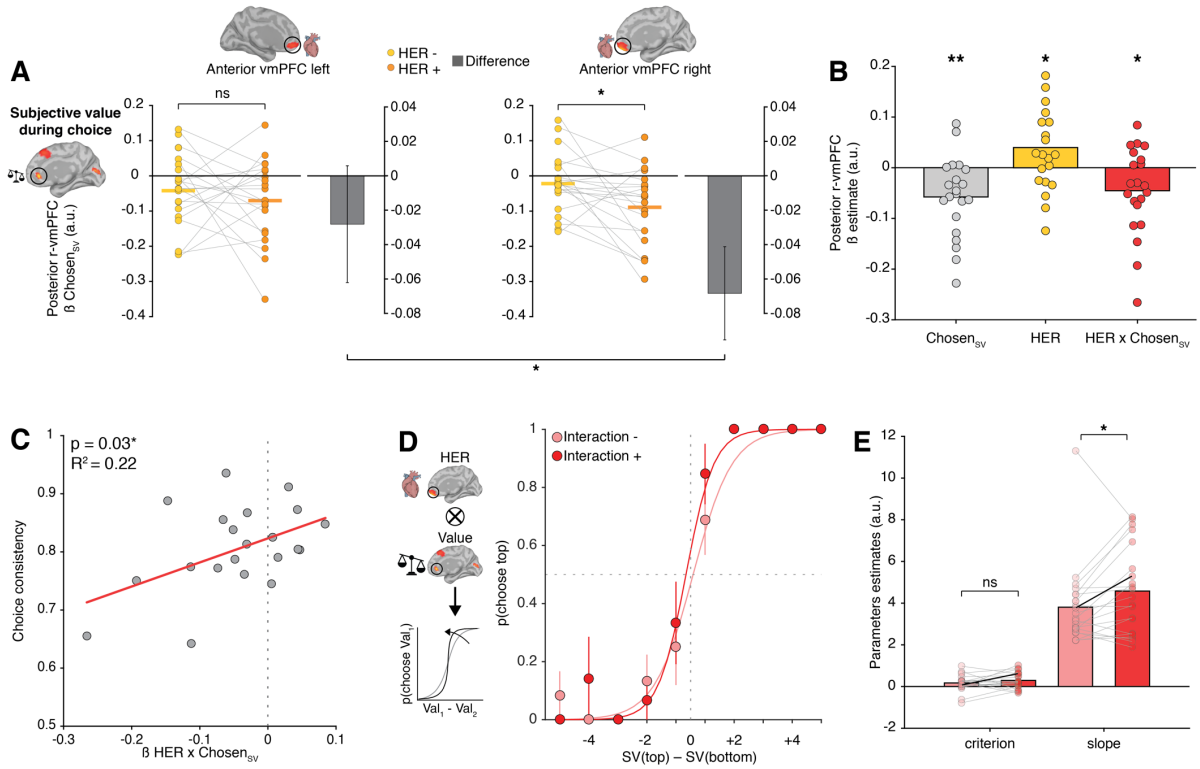

Fig. 3. The interaction between HER and value encoding accounts for inter-individual variability in choice consistency and for intra-individual trial-by-trial fluctuations of choice precision. A, Parameter estimates for the encoding of the chosen option value in posterior r-vmPFC during choice, in trials where HERs during task preparation were small (yellow) or large (orange) in left anterior vmPFC (left), or in right anterior vmPFC (right). Each dot represents a participant, the horizontal line indicates the mean. The difference in value encoding between large and small HER (grey bars; error bars indicate SEM) was significant in right vmPFC (ANOVA on value encoding, significant interaction HER amplitude x hemisphere, $F_{(1,40)}$=5.07 p=0.036); two tailed paired t-test comparing encoding strength for trials with large or small HERs in right vmPFC, $t_{(20)}$=2.52 p=0.02) **B**, Activity in posterior r-vmPFC is by design explained by the chosen option subjective value, but it is also explained by HER amplitude in anterior r-vmPFC during instructions and by the interaction between HER and value encoding. **C,** Robust regression shows that the magnitude of the interaction between HER and value encoding positively predicts inter-individual variability in choice consistency **D,** Behavioral data (dots) and fitted psychometric function (lines) for one representative participant, in trials with a large or small interaction between HER and value encoding. Error bars represent SEM. **E**, Criterion and slope of the psychometric function in all participants, revealing a significantly steeper slope for trials with large interaction between HER and value-related vmPFC activity (p = 0.037). Decision criterion is unaffected. Black lines represent the parameters estimates of the participant displayed in D. *p<0.05, **p<0.01.

236 The interaction between HER amplitude and subjective value encoding in right vmPFC was
237 further tested using a full parametric approach. Here (GLM2), we predicted the activity of posterior r-
238 vmPFC during choice from the subjective value of the chosen option, the HER amplitude in anterior r-
239 vmPFC during instruction period and the interaction between these two terms (**Fig. 3B**). Since the
240 posterior vmPFC region of interest was defined based on its encoding of the chosen value, the parameter
241 estimate for chosen value was, as expected, large ($ß_{ChosenSV}$ = -0.06 ± 0.02, two-tailed t-test against 0,
242 $t_{(20)}$ = -3.37, p = 0.003). Activity in posterior vmPFC was also predicted by the amplitude of HERs
243 occurring about 1.5 s earlier, during the instruction period, independently from the chosen value ($ß_{HER}$
244 = 0.04 ± 0.02, two-tailed t-test against 0, $t_{(20)}$= 2.13, p = 0.046), and importantly by the interaction
245 between HERs and chosen value ($ß_{HER* ChosenSV}$ = -0.05 ± 0.02, two-tailed t-test against 0, $t_{(20)}$= -2.41, p
246 = 0.025). Both the median-split analysis and the parametric model thus reveal a significant interaction
247 between the amplitude of HERs during instruction period and the neural encoding of subjective value
248 during choice.
249
250 We then verified that the effect on the neural encoding of subjective value was specific to HER
251 amplitude, and not due to an overall baseline shift in anterior r-vmPFC during the instruction period.
252 We ran an alternative model (GLM3) in which the activity in posterior r-vmPFC was predicted from
253 the subjective value of the chosen option, the activity in anterior r-vmPFC averaged during the whole
254 instruction period, i.e. activity not time-locked to heartbeats, and the interaction between the two terms.
255 This analysis revealed that while the subjective value of the chosen option still significantly predicted
256 the activity of posterior r-vmPFC ($ß_{ChosenSV}$ = -0.05 ± 0.02, two-tailed t-test against 0, $t_{(20)}$ = -3.27, p =
257 0.004), the other two terms did not (activity in anterior r-vmPFC averaged during instruction period:
258 $ß_{BL\ vmPFC}$ = 0.006 ± 0.03, two-tailed t-test against 0, $t_{(20)}$ = 0.22, p = 0.83, BF = 0.25; interaction: $ß_{BL}$
259 $_{vmPFC* ChosenSV}$ -0.03 ± 0.02, two-tailed t-test against 0, $t_{(20)}$ = -1.55, p = 0.14, BF = 1.14). The encoding
260 of subjective value is thus specifically modulated by HER amplitude in anterior r-vmPFC and not by
261 an overall baseline shift unrelated to heartbeats in the same region.

262 The functional coupling between HERs and subjective value encoding was also region specific:
263 HER amplitude in anterior r-vmPFC did not modulate the strength of value encoding in any other value-
264 related regions (dmPFC, occipital poles and posterior insula; all $p \geq 0.13$, all $BF \leq 0.81$; **Supplementary**
265 **Table 6**). Conversely, HERs outside anterior r-vmPFC did not significantly interact with value
266 encoding in posterior r-vmPFC. Splitting trials based on the amplitude in the two other cortical regions
267 showing differential heartbeats-evoked responses (**Fig. 2C**) showed no significant modulation of value
268 encoding in right posterior vmPFC (post-central complex: two-tailed paired t-test, $t_{(20)} = -1.41$, $p = 0.17$,
269 $BF = 0.90$; right supramarginal gyrus: two-tailed paired t-test, $t_{(20)} = -1.96$, $p = 0.06$, $BF = 2.41$).
270
271
272 **The interaction between HER and value encoding predicts choice consistency**
273 To what extent does the interaction between HER and value encoding in vmPFC predict
274 behavior? We first tested whether the interaction between HER and value encoding relates to inter-
275 individual differences in choice consistency, i.e. whether participants selected the movie to which they
276 had attributed the greatest likeability rating the day before. Given the overall high consistency in
277 preference-based decisions, which may reduce our ability to detect significant relationships, we
278 computed mean choice consistency using the top-50% most difficult trials (i.e. trials above median
279 difficulty in each participant). We regressed the model parameter of the interaction between HER and
280 value encoding ($ß_{HER*ChosenSV}$ obtained from GLM2) against mean choice consistency across
281 participants. The larger the interaction between HER and value encoding, the more consistent were
282 participants in their choices ($ß_{robust} = 0.41$, robust regression $R^2 = 0.22$, $t_{(19)} = 2.29$, $p = 0.03$; **Fig. 3C**).
283 In other words, 22% of inter-individual difference in behavioral consistency is explained by the
284 magnitude of the interaction between HER and value encoding.
285 The correlation between neural activity and behavior was specific to the interaction parameter:
286 inter-individual differences in choice consistency could not be predicted from the model parameter
287 estimate of HER ($ß_{HER}$ from GLM2; $ß_{robust} = 0.02$, $R^2 = 4*10^{-4}$, $t_{(19)} = 0.09$, $p = 0.93$, $BF = 0.39$), nor
288 from the parameter estimate of value ($ß_{ChosenSV}$ from GLM2; $ß_{robust} = -0.19$, $R^2 = 0.04$, $t_{(19)} = -0.88$, p =

289 0.39, BF = 0.52). None of the personality traits tested nor interoceptive ability, assessed with the
290 heartbeat counting task, significantly co-varied with the interaction between HER and subjective value
291 encoding (**Supplementary Table 7**).
292
293 So far, results are based on parameter estimates computed across trials for a given participant.
294 To assess how within-participant trial-by-trial fluctuations in behavior relates to the interaction between
295 HERs and subjective value encoding, we computed the z-scored product of the HER amplitude in
296 anterior r-vmPFC during the instruction period and the value-related activity in posterior r-vmPFC
297 during choice. We then median-split the trials according to this product and modeled participants'
298 choices separately for trials with a small vs. large interaction (**Fig. 3D**). When the interaction was large,
299 psychometric curves featured a steeper slope, corresponding to an increased choice precision (two-
300 tailed paired t-test, $t_{(20)}$= -2.24, p = 0.037, Cohen's d = -0.49; after removal of the unique outlier with a
301 slope estimate exceeding 3 SD from population mean, $t_{(19)}$ = -3.30, p = 0.003, Cohen's d= -0.74; **Fig.**
302 **3E**), while decision criterion was not affected (two-tailed paired t-test, $t_{(20)}$= -1.20, p = 0.25, BF = 0.64;
303 after outlier removal $t_{(19)}$ =-0.96, p = 0.35, BF = 0.46; **Fig. 3E**).
304 To control for the specificity of the interaction, we estimated the psychometric function on trials
305 median-split on HER amplitude alone but found no difference in choice precision (two-tailed paired t-
306 test, $t_{(20)}$= 0.41, p = 0.69, BF = 0.27) nor in criterion (two-tailed paired t-test, $t_{(20)}$= 0.52, p = 0.61, BF =
307 0.29). Similarly, median-splitting trials on value-related posterior r-vmPFC activity alone revealed no
308 difference in the psychometric curve (two-tailed paired t-test, slope, $t_{(20)}$= 0.21, p = 0.84, BF = 0.25;
309 criterion: $t_{(20)}$= -0.57, p = 0.58, BF = 0.30). Therefore, our results indicate that trial-by-trial choice
310 precision is specifically related to the interaction between HERs in anterior r-vmPFC and value-related
311 activity in posterior r-vmPFC.
312 Altogether, these results indicate that the interaction between HER amplitude and subjective
313 value encoding accounts both for within-subject inter-trial variability, and for inter-individual
314 differences in preference-based choice consistency.
315

316 **HER effects are specific to preference-based choices**

317 Finally, we tested whether the effect of HER was specific to subjective value or whether it is a more
318 general mechanism interacting with all types of decision-relevant evidence. To this aim, we analyzed
319 perceptual discrimination trials using the same approach as for preference-based trials. First, we
320 modeled the single trial response-locked MEG sensor-level data using a GLM (GLM1b) with the
321 parameters accounting for choice in the perceptual task (i.e. contrast of the chosen option – $Chosen_{Ctrs}$
322 – and the contrast of the unchosen option – $Unchosen_{Ctrs}$), as well as response button. We then identified
323 the time windows where the contrast of the chosen option, unchosen option and response button were
324 encoded (**Supplementary Table 8**) and determined the cortical regions contributing to the encoding of
325 the contrast of the chosen option (**Supplementary Fig. 2, Supplementary Table 9**). Finally, we
326 median-split perceptual trials according to the amplitude of HERs in anterior r-vmPFC. The encoding
327 strength of the contrast of the chosen option did not interact with heart-evoked responses amplitude in
328 any of the contrast-encoding regions (all $p \geq 0.26$, $BF \leq 0.62$; **Supplementary Table 10**). The results
329 thus indicate that HER amplitude in r-vmPFC is specifically linked to the cortical encoding of subjective
330 value.

Discussion

Preparing for subjective preference-based decisions led to larger responses to heartbeats in vmPFC, as expected from previous studies relating self and HERs (11–13), and in post-central gyrus, a region known to respond to heartbeats (4, 10, 18). We further reveal that HERs before option presentation interact specifically with subjective value encoding during choice in vmPFC. The interaction between HERs and value encoding predicted preference-based choices: it was associated to more precise decisions at the single trial level, and predicted inter-individual variability in choice consistency over time. No interaction between HER and the encoding of perceptual evidence could be found in the control objective task. Neither the HER difference between the two tasks, nor the interaction between HER and value in the subjective preference task, could be trivially explained by changes in cardiac parameters (heart rate, heart rate variability, ECG, stroke volume) nor by changes in arousal state (pupil diameter, alpha power). Altogether, our results reveal how the self-reflection intrinsic to preference-based decisions involves the neural read-out of a physiological variable and its integration in the subjective valuation process.

In line with previous studies relating the self with HERs in vmPFC (11–13), we find that HERs are more pronounced when preparing for the subjective preference task than when preparing for the objective discrimination task. A number of self-related processes might take place specifically when preparing for the subjective preference-based task, such as turning attention inward or pre-activating autobiographical memory circuits. Note that HERs cannot be influenced by processes triggered by the movie titles themselves, such as retrieving movie-specific information from memory, since options are not yet available in the instruction period where HERs are measured. HERs were not associated with any change in the neural encoding of objective perceptual evidence. This result might seem at odds with previously reported effects of HERs on sensory detection at threshold (13, 18). However, as opposed to the perceptual discrimination task used here, sensory detection at threshold is intrinsically subjective, since participants are asked to introspect and report their fluctuating subjective experience in response to physically and objectively constant stimuli (19, 20). Last, there was no difference in cardiac

358 parameters between the two tasks. Our results thus differ from previous observations in risky decisions,
359 where changes in peripheral bodily signals predicted behavioral performance (21). More generally, this
360 indicates that HER fluctuations relevant for valuation and behavior correspond to changes in the quality
361 of the neural monitoring in cardiac inputs, rather than to changes in cardiac activity.
362
363 We successfully retrieved with MEG the cortical valuation network described in the fMRI
364 literature (16, 22, 23), including dmPFC and vmPFC, during the choice period. These findings are
365 interesting *per se*, as data on the temporal course of value-based choices in the human prefrontal cortex
366 remain scarce (24–26). Here, we find that chosen value is robustly encoded in the valuation network
367 from 600 ms to 200 ms before motor response, with a temporal (but not spatial) overlap with motor
368 preparation. Note that we did not find a robust encoding of the unchosen value, in line with
369 electrophysiological recordings in the monkey orbitofrontal cortex where the encoding of the chosen
370 value dominates (25, 27–29). Chosen value encoding interacted with HERs specifically in vmPFC, a
371 region shown by separate streams of studies to play a role in valuation (30–32) and self-related cognition
372 (33, 34), but long suspected to play an integrative role in decision making (35). In the objective
373 discrimination task, perceptual-relevant evidence was encoded, among other regions, in posterior
374 parietal cortex, consistent with monkey electrophysiology literature (36, 37).
375
376 Because fluctuations in HERs occurred during task preparation, before option presentation,
377 their influence on value encoding might generally pertain to the interaction between ongoing activity
378 (during task preparation) and stimulus-evoked activity (in response to option presentation). HERs
379 constitute a very specific subset of such interaction: HERs interacted only with value, but not with
380 visual evoked responses for instance, and only in vmPFC in the subjective task. Conversely, no
381 interaction between overall ongoing activity in vmPFC and value encoding could be found. Besides,
382 HERs modulated value encoding in a multiplicative manner. Our results thus differ from a previously
383 reported vmPFC baseline-shift additive effect in pleasantness ratings (38, 39). Altogether, our results
384 indicate that part of the unspecified 'neural noise' driving fluctuations in choice consistency (40–42)

comes from the interaction between interoceptive self-related processes, indexed by neural monitoring of cardiac signals, and the neural encoding of subjective value. A more detailed mechanistic account of how responses to heartbeat during task preparation influence the subjective valuation process taking place about 1.5 second later remains to be established. Still, our results pave the way for the quantification of self-related processes in decision making, an aspect mostly absent from computational models of decision-making despite its relevance to understand maladaptive decisions in psychiatric disorders (8, 43, 44).

Decisions on primary goods such as food integrate information about internal bodily states to select options that preserve the integrity of the organism that needs to be fed and protected – the simplest notion of self. We show here that the subjective valuation of cultural goods, that rely on the same cortical valuation network as employed for primary goods (15, 45–48), has inherited a functional link with the central monitoring of physiological variables. Even when choosing between cultural goods that do not fulfill any immediate basic need, the neural monitoring of heartbeats supports self-reflection underlying evaluation, contributing to the precision of subjective decisions and fostering the stable expression of long-lasting preferences that define, at least in part, our identity.

401 # Methods

402

403 **Participants**

404 24 right-handed volunteers with normal or corrected-to-normal vision took part in the study after
405 having given written informed consent. They received monetary compensation for their participation.
406 The ethics committee CPP Ile de France III approved all experimental procedures. Three subjects
407 were excluded from further analysis: one subject for too low overall performance (74%, 2 standard
408 deviations below the mean = 87.6%), one subject was excluded for excessive number of artifacts
409 (29.7% of trials, above 2 standard deviations, mean = 7%), one subject was excluded because the ICA
410 correction of the cardiac artifact was not successful.
411 21 subjects were thus retained for all subsequent analyses (9 male; mean age: 23.57 ± 2.4 years; mean
412 ± SD).

413

414 **Tasks and procedure**

415 Participants came on two consecutive days to the lab (mean elapsed time between the two sessions
416 22.28 ± 3.55 hours) to complete two experimental sessions. The first session was a likability rating on
417 movies (behavior only), from which we drew the stimuli used in the second experimental session,
418 during which brain activity was recorded with magnetoencephalography (MEG).
419 *Rating session*. We selected 540 popular movies form the Web (allocine.fr) whose title maximal
420 length was 16 characters (spaces included). DVD covers and titles of the pre-selected movies were
421 displayed one by one on a computer screen and subjects had to indicate whether they had previously
422 watched the currently displayed movie by pressing a 'yes' or 'no' key on a computer keyboard, without
423 any time constraint (**Supplementary Fig. 1A**). Participants were then presented with the list of movie
424 titles they had previously watched and asked to name the 2 movies they liked the most and the two
425 they liked the least. Participants were explicitly instructed to use these 4 movies as reference points
426 (the extremes of the rating scale) to rate all other movies. Last, the titles and the covers of the movies
427 belonging to the list were displayed one by one at the center of the computer screen in random order.

Participants assigned to each movie a likability rating by displacing (with arrow keys) a cursor on a 21-points Likert scale and validated their choice with an additional button press (**Supplementary Fig. 1B**). Likability ratings were self-paced and the starting position of the cursor was randomized at every trial.

Stimuli. Experimental stimuli consisted of 256 pairs of written movie titles drawn from the list of movies that each participant had rated on the first day. Each movie title was characterized along two experimental dimensions: its likability rating (as provided by the participant) and its contrast. The mean contrast was obtained by averaging the luminance value (between 40 and 100; grey background at 190) randomly assigned to each character of the title. We manipulated trials difficulty by pairing movie titles so that the differences between the two items along the two dimensions (i.e., likability and contrast) were parametric and orthogonal. Additionally, we controlled that the sum of ratings and the sum of contrast within each difficulty level was independent of their difference and evenly distributed. Each pair of stimuli was presented twice in the experiment: one per decision type. A given movie title could appear in up to 10 different pairs. The position of the movie titles on the screen was pseudo-randomly assigned so that the position of the correct option (higher likeability rating or higher contrast) was fully counter-balanced.

Experimental task. On the second day, subjects performed a two-alternative forced-choice (2AFC) task while brain activity was recorded with MEG. At each trial, participants were instructed to perform one of the two decisions types on the pair of movie titles (**Fig. 1A**): either a preference decision, in which they had to indicate the item they liked the most, or a perceptual discrimination, in which they had to indicate the title written with the higher contrast. Each trial began with a fixation period of variable duration (uniformly distributed between 0.8 and 1.2 seconds in step of 0.05 s) indicated by a black fixation dot surrounded by a black ring (internal dot, 0.20° of visual angle; external black ring, 0.40° of visual angle), starting from which participants were required not to blink anymore. Next, the outer ring of the fixation turned either into a square or a diamond (0.40° and 0.56° visual angle, respectively) indicating which type of decision participants were to perform (preference-based or perceptual, counter-balanced across participants), for 1.5 seconds. Then, the outer shape

turned again into a ring and two movie titles appeared above and below it (visual angle 1.09°). Options remained on screen until response was provided (via button press with the right hand) or until 3 seconds had elapsed. After response delivery, movie titles disappeared and the black fixation dot surrounded by the black circle remained on screen for 1 more second. The central dot turned green and stayed on screen for variable time (uniformly distributed between 2.5 and 3 seconds in step of 0.05 s), indicating participants that they were allowed to blink before the beginning of next trial. Each recording session consisted of 8 blocks of 64 trials each.

Prior to the recording session, participants familiarized themselves with the experimental task by carrying out 3 training blocks. The first 2 blocks (10 trials each) comprised trials of one type only, hence preceded by the same cue symbol. The last block contained interleaved trials (n=20), as in the actual recording. The movie pairs used during training were not presented again during the recording session.

Heartbeat counting task. After performing the 8 experimental blocks, we assessed participants' interoceptive abilities by asking them to count their heartbeats by focusing on their bodily sensations, while fixating the screen (49). Subjects performed six blocks of different durations (30, 45, 60, 80, 100, 120 seconds) in randomized order. No feedback on performance was provided. Since the acquisition of our dataset, this widely used paradigm has been criticized in several respects (50–52).

Questionnaires. Once subjects left the MEG room, they filled 4 questionnaires in French: Beck's Depression Inventory (BDI) (53), Peter's et al. Delusions Inventory (PDI) (54), the Trait Anxiety Inventory (STAI) (55) and the Obsessive-Compulsive Inventory (OCI) (56).

Recordings

Neural activity was continuously recorded using a MEG system with 102 magnetometers and 204 planar gradiometers (Elekta Neuromag TRIUX, sampling rate 1000 Hz, online low-pass filter at 330 Hz). Cardiac activity was simultaneously recorded (BIOPAC Systems, Inc.; sampling frequency 1000 Hz; online filter 0.05-35 Hz). The electrocardiogram was obtained from 4 electrodes (2 placed in over the left and right clavicles, 2 over left and right supraspinatus muscles (57)) and referenced to another

electrode on the left iliac region of the abdomen, corresponding to four vertical derivations. The four horizontal derivations were computed offline by subtracting the activity of two adjacent electrodes. Additionally, we measured beat-to-beat changes in cardiac impedance, to compute the beat-by-beat stroke volume (i.e. the volume of blood ejected by the heart at each heartbeat (58)). Impedance cardiography is a non-invasive technique based on the impedance changes in the thorax due to the changes in fluid volume (blood). A very low-intensity (400 μA rms) high frequency (12.5 kHz) electric current was injected via two source electrodes: the first one was placed on the left side of the neck and the second 30 cm below it (roughly on the sixth rib). Two other monitoring electrodes (placed 4 cm apart from the source ones: below the source electrode on the neck and above the source electrode on the rib cage) measured the voltage across the tissue. To determine left ventricular ejection time, aortic valve activity was recorded by placing an a-magnetic homemade microphone (online band-pass filter 0.05-300 Hz) on the chest of the subject.

Pupil diameter and eye movements were tracked using an eye-tracker device (EyeLink 1000, SR Research) and 4 electrodes (2 electrodes placed on the left and right temples and 2 electrodes placed above and below participant's dominant eye).

Cardiac events and parameters

Cardiac events were detected on the right clavicle-left abdomen ECG derivation in all participants. We computed a template of the cardiac cycle, by averaging a subset of cardiac cycles, which was then convolved with the ECG time series. R-peaks were identified as peaks of the result of the convolution, normalized between 0 and 1, exceeding 0.6. All other cardiac waves were defined with respect R-peak. In particular, T-waves were identified as the maximum amplitude occurring within 420 milliseconds after the Q-wave. R-peak and T-wave automatic detection was visually verified for each participant.

Inter-beat intervals (IBIs) were defined for each phase of the trial as the intervals between two consecutive R-peaks. More specifically, we considered for 'fixation', 'instruction period' and 'response' phases the two R-peaks around their occurrence. IBIs during 'choice' were based on the

two R-peaks preceding response delivery. Inter-beat variability was defined as the standard deviation across trials of IBIs in a given trial phase.

Stroke volume was computed according to the formula (58, 59):

$$SV = \rho \times \left(\frac{L^2}{Zo^2}\right) \times LVET \times \frac{dZ}{dT_{(max)}}$$

where ρ is the resistivity of the blood (135 Ohms*cm) (60), L^2 is the distance between the two source electrodes, Zo^2 is the base impedance, $LVET$ is the systolic left ventricular ejection time (in seconds), $dZ/dT_{(max)}$ is the largest impedance change during systole (Ohms/sec). Note that because we obtained stroke volume by injecting a current at 12.5 kHz, rather than the more typical frequency of 100 kHz, absolute stroke volumes are systematically underestimated, but relative values are preserved.

MEG data preprocessing

External noise was removed from the continuous data using MaxFilter algorithm. Continuous data were then high-pass filtered at 0.5 Hz (4th order Butterworth filter). Trials (defined as epochs ranging from fixation period to 1 second after response) contaminated by muscle and movement artifacts were manually identified and discarded from further analyses (6% of trials on average, ranging from 0% to 15%).

Independent component analysis (ICA) (61), as implemented in FieldTrip Toolbox (62) was used to attenuate the cardiac artifact on MEG data. ICA was computed on MEG data epoched ±200 ms around the R-peak of the ECG, in data segments that were free of artifacts, blinks and saccades above 3 degrees. The number of independent components to compute was set to be equal to the rank of the MEG data. Mean pairwise phase consistency (PPC) was estimated for each independent component (63) with the right clavicle-left abdomen ECG derivation signal in the frequency band 0-25 Hz. Components (up to 3) that exceeded 3 standard deviations from mean PPC were then removed from the continuous data.

To correct for blinks, 2-seconds segments of data were used to estimate blink and eye-movement components. Mean PCC was then computed with respect to vertical EOG signal, and components exceeding mean PCC + 3 standard deviations were removed from continuous data. The procedure was iterated until no component was beyond 3 standard deviations or until 3 components in total were removed. Stereotypical blink components were manually selected in two participants as the automated procedure failed to identified them.

ICA-corrected data were then low-pass filtered at 25 Hz (6th order Butterworth filter)

Trials selection

Trials had to meet the following criteria to be included in all subsequent analysis: no movement artifacts, sum of blinking periods less than 20% of total trial time, at least one T-peak during instruction period (cf. HERs section), and reaction time neither too short (at least 250 ms) nor too long. To identify exceedingly long RTs, we binned the trials of each task in 4 difficulty levels based on the difference of the two options (i.e., difference in ratings in preference-based choice and difference in contrast for the perceptual ones). Within each difficulty level, for correct and error trials separately, we excluded the trials with reaction times exceeding the participant's mean RT + 2 standard deviations.

The average number of trials retained per participant was 421.67 ± 43.36 (mean ± SD).

Heartbeat evoked responses

Heart-evoked responses were computed on MEG data time-locked to T-wave occurring during the instruction period. T-waves had to be at minimum 400 ms distance from the subsequent R-peak. In order to avoid contamination by transient visual responses or by preparation to the subsequent visual presentation, we only retained T-waves that occurred at least 300 milliseconds after the onset of the instruction cue and 350 milliseconds before the onset of options presentation. If more than one T-wave occurred in this period, HERs for that trial were averaged. HERs were analyzed from T-wave + 50 ms to minimize contamination by the residual cardiac artifact (64) after ICA correction.

We verify that differences in HERs between the two types of decision were truly locked to heartbeats, and that a difference of similar magnitude could not arise by locking the data to any time point of the instruction period. To this end, we created surrogate timings for heartbeats (within the instruction period), to break the temporal relationship between neural data and heartbeats, and computed surrogate HERs. We created 500 surrogate heartbeat data set, by permuting the timings of the real T-wave between trials belonging to the same decision type (i.e., the timing of the T-wave at trial *i* was randomly assigned to trial *j*). We then searched for surrogate HER differences between trial types using a cluster-based permutation test (17) (see below). For each of the 500 iterations, we retained the value of the largest cluster statistics (sum(t)) to estimate the distribution of the largest difference that could be obtained randomly sampling ongoing neural activity during the same instruction period. To assess statistical significance, we compared the cluster statistics from the original data against the distribution of surrogate statistics.

Nonparametric statistical testing of MEG data

HERs difference between preference-based and perceptual trials during instruction presentation was tested for statistical significance using cluster-based permutation two-tailed t-test (17) as implemented in FieldTrip toolbox (62), on magnetometer activity in the time-window 50-300 ms after T-wave. This method defines candidate clusters of neural activity based on spatio-temporal adjacency exceeding a statistical threshold ($p < 0.05$) for a given number of neighboring sensors (n=3). Each candidate cluster is assigned a cluster-level test statistics corresponding to the sum of *t* values of all samples belonging to the given cluster. The null distribution is obtained non-parametrically by randomly shuffling conditions labels 10,000 times, computing at each iteration the cluster statistics and saving the largest positive and negative *t* sum. Monte Carlo p value corresponds to the proportion of cluster statistics under the null distribution that exceed the original cluster-level test statistics. Because the largest chance values are retained to construct the null distribution, this method intrinsically corrects for multiple comparisons across time and space. Controls analyses involving the clustering procedure were performed with the same parameters.

The significance of beta time-series obtained from GLM analyses at the sensor level was obtained using cluster-based permutation two-tailed t-test against zero.

Bayes factor

We used Bayes factors (BF) to quantify the evidence in support of the null hypothesis (H_0 = no difference between 2 measures). To this aim, we computed the maximum log-likelihood of a gaussian model in favor of the alternative hypothesis and for the model favoring the null adjusting the effect size to correspond to a p = 0.05 for our sample size (n = 21 for all analyses except for pupil for which n = 16 and for 3 ECG derivations for which n=20). Finally, we computed Bayesian information criterion and the corresponding Bayes factor. As a summary indication, BF < 0.33 provides substantial evidence in favor of the null hypothesis, BF between 0.33 and 3 does not provide enough evidence for or against the null (65).

For regression analyses, Bayes Factor was computed using the online calculator tool (http://pcl.missouri.edu/bf-reg) based on Liang and colleagues (66).

Generalized linear model on response-locked single trials

To analyze how task-related variables are encoded in neural activity during decision, we ran a generalized linear model (GLM) on baseline-corrected (-500 to -200 ms before instruction presentation) single trial MEG data time-locked to button press. We predicted z-scored MEG activity at each time-point and channel using task-relevant experimental variables. For preference-based decisions we modeled MEG activity as:

$$MEG_{t,c} = \beta_0 + \beta_{ChosenSV} + \beta_{UnchosenSV} + \beta_{Button\ press} \quad (GLM1a)$$

where *t* and *c* represent MEG activity at time-point *t* at channel *c*, β_0 is the intercept, $\beta_{ChosenSV}$ are the z-scored ratings of the chosen option, $\beta_{UnchosenSV}$ is the z-scored rating of the alternative unchosen option and $\beta_{Button\ press}$ is a categorical variable representing motor response (i.e. top or bottom). Similarly, for perceptual decisions we used:

$$MEG_{t,c} = \beta_0 + \beta_{ChosenCtrs} + \beta_{UnchosenCtrs} + \beta_{Button\ press}\ (GLM1b)$$

where $\beta_{ChosenCtrs}$ and $\beta_{UnchosenCtrs}$ are the z-scored contrast of the chosen and unchosen option, respectively.

This procedure provided us with time series of beta values at each channel that could be tested against zero for significance using spatio-temporal clustering (17). Once significant clusters encoding task-related variables were identified at the sensor level, we reconstructed the cortical sources corresponding to the sensor-level activity averaged within the significant time-window. We modeled source-reconstructed neural activity with the same GLMs to identify the cortical areas mostly contributing to the significant sensor-level effect.

Generalized linear model on posterior right vmPFC

To quantify the influence of HER in anterior r-vmPFC during instructions on subjective value encoding during choice, we modeled the activity of posterior r-vmPFC, encoding subjective value with the following GLM:

$$Posterior\ r\text{-}vmPFC = \beta_0 + \beta_{Chosen\mathrm{SV}} + \beta_{HER} + \beta_{\mathrm{HER*ChosenSV}}\ (GLM2)$$

where, β_0 is the intercept, $\beta_{Chosen\mathrm{SV}}$ are the z-scored ratings of the chosen option, β_{HER} is the z-scored activity in the anterior right vmPFC cluster defined by comparing HERs in preference-based vs. perceptual choices and $\beta_{Chosen\mathrm{SV*HER}}$ is the interaction term obtained by multiplying the z-scored previous predictors.

To verify that the interaction between subjective value encoding and HER amplitude was specifically time-locked to heartbeats and not a general influence of baseline activity in anterior r-vmPFC, we ran an alternative model to explain posterior r-vmPFC activity:

$$Posterior\ r\text{-}vmPFC = \beta_0 + \beta_{Chosen\mathrm{SV}} + \beta_{BL\ vmPFC} + \beta_{BL\ vmPFC*ChosenSV}\ (GLM3)$$

642 where, β_0 is the intercept, $\beta_{ChosenSV}$ are the z-scored ratings of the chosen option, $\beta_{BL\ vmPFC}$ is the z-
643 scored activity in anterior r-vmPFC during instructions averaged across the whole instruction period,
644 not time-locked to heartbeats and $\beta_{BL\ vmPFC*ChosenSV}$ is the interaction between the two preceding
645 predictors. Note that regressors are not orthogonalized in any of the GLMs.
646
647 **Anatomical MR acquisition and preprocessing**
648 An anatomical T1 scan was acquired for each participant on a 3 Tesla Siemens TRIO (n = 2) or
649 Siemens PRISMA (n = 20) or Siemens VERIO (n = 2). Cortical segmentation was obtained by using
650 automated procedure as implemented in the FreeSurfer software package (67). The results were
651 visually inspected and used for minimum-norm estimation.
652
653 **Source reconstruction**
654 Cortical localization of neural activity was performed with BrainStorm toolbox (68). After co-
655 registration of individual anatomy and MEG sensors, 15,003 current dipoles were estimated using a
656 linear inverse solution from time-series of magnetometers and planar gradiometers (weighted
657 minimum-norm, SNR of 3, whitening PCA, depth weighting of 0.5) using overlapping-spheres head
658 model. Current dipoles were constrained to be normally oriented to cortical surface, based on
659 individual anatomy. Source activity was obtained by averaging sensor-level time-series in the time-
660 windows showing significant effects (difference between HERs and beta values different from zero),
661 spatially smoothed (FWHM 6 mm) and projected onto standard brain model (ICBM152_T1, 15,003
662 vertices). Note that sources in subcortical regions cannot be retrieved with the reconstruction method
663 used here.
664 To assess which cortical areas contributed the most to the effects observed at the sensor-level, we ran
665 parametric two-tailed t-test and reported all clusters of activity spatially extending more than 20
666 vertices with individual t-values corresponding to $p < 0.005$ (uncorrected for multiple comparisons).
667 We reported the coordinates of vertices with the maximal t value and their anatomical labels
668 according to AAL atlas (69). For clusters falling into prefrontal cortices, we reported the

corresponding areas according to the connectivity-based parcellation developed by Neubert and colleagues (70).

Pupil data analysis

Pupil data that contained blinks (automatically detected with EyeLink software and extended before and after by 150 ms), saccades beyond 2 degrees and segments in which pupil size changed abruptly (signal temporal derivative exceeding 0.3, arbitrary unit) were linearly interpolated. All interpolated portions of the data that exceeded 1 second were removed from further analyses. Continuous pupil data from each experimental block were then band-pass filtered between 0.01 and 10 Hz (second order Butterworth) and z-scored. 16 subjects were retained for pupil analysis; 5 subjects were excluded due to too low quality of data. Pupil analysis was performed in two ways: 1) averaged pupil diameter in the same time period used for HER computation (i.e., 300 ms after instruction presentation until 350 ms before options display) and 2) averaged pupil diameter in the time-window spanning 1 second before button press until its execution.

Acknowledgements

The authors thank Clémence Alméras, Maximilien Chaumon and Christophe Gitton for assistance in data acquisition.

This work was supported by funding from the European Research Council (ERC) under the European Union's Horizon 2020 research and innovation program (grant agreement No 670325, Advanced grant BRAVIUS) and a senior fellowship of the Canadian Institute For Advance Research (CIFAR) program in Brain, Mind and Consciousness to CTB; by a grant from the Ecole des Neurosciences de Paris Ile de France to DA; and by ANR-17-EURE-0017.

References:

1. A. R. Damasio, *Self Comes to Mind: Constructing the Conscious Brain* (Pantheon Books, 2010).
2. H.-D. Park, C. Tallon-baudry, The neural subjective frame: from bodily signals to perceptual consciousness. *Philos. Trans. R. Soc. Lond. B. Biol. Sci.* **369**, 20130208 (2014).
3. O. Blanke, T. Metzinger, Full-body illusions and minimal phenomenal selfhood. *Trends Cogn. Sci.* **13**, 7–13 (2009).
4. D. Azzalini, I. Rebollo, C. Tallon-Baudry, Visceral Signals Shape Brain Dynamics and Cognition. *Trends Cogn. Sci.* **23**, 488–509 (2019).
5. A. D. Craig, How do you feel? Interoception: the sense of the physiological condition of the body. *Nat. Rev. Neurosci.* **3**, 655–666 (2002).
6. M. Keramati, B. Gutkin, Homeostatic reinforcement learning for integrating reward collection and physiological stability. *Elife* **3**, 1–26 (2014).
7. K. Juechems, C. Summerfield, Where does value come from? *Trends Cogn. Sci.*, 836–850 (2019).
8. M. P. Paulus, Decision-Making Dysfunctions in Psychiatry—Altered Homeostatic Processing? *Science (80-.).* **318**, 602–606 (2007).
9. P. Montoya, R. Schandry, A. Müller, Heartbeat evoked potentials (HEP): topography and influence of cardiac awareness and focus of attention. *Electroencephalogr. Clin. Neurophysiol. Evoked Potentials* **88**, 163–172 (1993).
10. M. Kern, A. Aertsen, A. Schulze-Bonhage, T. Ball, Heart cycle-related effects on event-related potentials, spectral power changes, and connectivity patterns in the human ECoG. *Neuroimage* **81**, 178–190 (2013).
11. M. Babo-Rebelo, C. G. Richter, C. Tallon-Baudry, Neural Responses to Heartbeats in the Default Network Encode the Self in Spontaneous Thoughts. *J. Neurosci.* **36**, 7829–7840 (2016).
12. M. Babo-Rebelo, N. Wolpert, C. Adam, D. Hasboun, C. Tallon-Baudry, Is the cardiac

721 monitoring function related to the self in both the default network and right anterior insula?
722 *Philos. Trans. R. Soc. B Biol. Sci.* **371**, 20160004 (2016).
723 13. H.-D. Park, S. Correia, A. Ducorps, C. Tallon-Baudry, Spontaneous fluctuations in neural
724 responses to heartbeats predict visual detection. *Nat. Neurosci.* **17**, 612–8 (2014).
725 14. M. Grueschow, R. Polania, T. A. Hare, C. C. Ruff, Automatic versus Choice-Dependent Value
726 Representations in the Human Brain. *Neuron* **85**, 874–885 (2015).
727 15. M. Lebreton, S. Jorge, V. Michel, B. Thirion, M. Pessiglione, An Automatic Valuation System
728 in the Human Brain: Evidence from Functional Neuroimaging. *Neuron* **64**, 431–439 (2009).
729 16. O. Bartra, J. T. McGuire, J. W. Kable, The valuation system: A coordinate-based meta-
730 analysis of BOLD fMRI experiments examining neural correlates of subjective value.
731 *Neuroimage* **76**, 412–427 (2013).
732 17. E. Maris, R. Oostenveld, Nonparametric statistical testing of EEG- and MEG-data. *J.*
733 *Neurosci. Methods* **164**, 177–190 (2007).
734 18. E. Al, *et al.*, Heart-brain interactions shape somatosensory perception and evoked potentials.
735 *Proc. Natl. Acad. Sci. U. S. A.* **117**, 10575–10584 (2020).
736 19. D. Ress, D. J. Heeger, Neuronal correlates of perception in early visual cortex. *Nat. Neurosci.*
737 **6**, 414–420 (2003).
738 20. F. Campana, C. Tallon-Baudry, Anchoring visual subjective experience in a neural model: The
739 coarse vividness hypothesis. *Neuropsychologia* **51**, 1050–1060 (2013).
740 21. A. Bechara, H. Damasio, D. Tranel, A. R. Damasio, Deciding Advantageously Before
741 Knowing the Advantageous Strategy. *Science (80-.).* **275**, 1293–1295 (1997).
742 22. J. A. Clithero, A. Rangel, Informatic parcellation of the network involved in the computation
743 of subjective value. *Soc. Cogn. Affect. Neurosci.* **9**, 1289–1302 (2014).
744 23. D. J. Levy, P. W. Glimcher, The root of all value: A neural common currency for choice. *Curr.*
745 *Opin. Neurobiol.* **22**, 1027–1038 (2012).
746 24. L. T. Hunt, *et al.*, Mechanisms underlying cortical activity during value-guided choice. *Nat.*
747 *Neurosci.* **15**, 470–476 (2012).

25. L. T. Hunt, T. E. J. Behrens, T. Hosokawa, J. D. Wallis, S. W. Kennerley, Capturing the temporal evolution of choice across prefrontal cortex. *Elife* **4**, 1–25 (2015).

26. R. Polanía, I. Krajbich, M. Grueschow, C. C. Ruff, Neural Oscillations and Synchronization Differentially Support Evidence Accumulation in Perceptual and Value-Based Decision Making. *Neuron* **82**, 709–720 (2014).

27. C. E. Strait, T. C. Blanchard, B. Y. Hayden, Reward value comparison via mutual inhibition in ventromedial prefrontal cortex. *Neuron* **82**, 1357–1366 (2014).

28. C. Padoa-Schioppa, J. A. Assad, Neurons in the orbitofrontal cortex encode economic value. *Nature* **441**, 223–226 (2006).

29. E. L. Rich, J. D. Wallis, Decoding subjective decisions from orbitofrontal cortex. *Nat. Neurosci.* **19** (2016).

30. L. K. Fellows, Deciding how to decide: Ventromedial frontal lobe damage affects information acquisition in multi-attribute decision making. *Brain* **129**, 944–952 (2006).

31. A. R. Vaidya, M. Sefranek, L. K. Fellows, Ventromedial Frontal Lobe Damage Alters how Specific Attributes are Weighed in Subjective Valuation. *Cereb. Cortex* **28**, 3857–3867 (2017).

32. M. R. Delgado, *et al.*, Viewpoints: Dialogues on the functional role of the ventromedial prefrontal cortex. *Nat. Neurosci.* **19**, 1545–1552 (2016).

33. J. R. Andrews-Hanna, J. Smallwood, R. N. Spreng, The default network and self-generated thought: Component processes, dynamic control, and clinical relevance. *Ann. N. Y. Acad. Sci.* **1316**, 29–52 (2014).

34. P. Qin, G. Northoff, How is our self related to midline regions and the default-mode network? *Neuroimage* **57**, 1221–1233 (2011).

35. A. R. Vaidya, L. K. Fellows, Under construction: ventral and lateral frontal lobe contributions to value-based decision-making and learning. *F1000Research* **9**, 1–8 (2020).

36. M. N. Shadlen, W. T. Newsome, Neural basis of a perceptual decision in the parietal cortex (area LIP) of the rhesus monkey. *J. Neurophysiol.* **86**, 1916–1936 (2001).

37. H. R. Heekeren, S. Marrett, L. G. Ungerleider, The neural systems that mediate human perceptual decision making. *Nat. Rev. Neurosci.* **9**, 467–479 (2008).

38. A. Lopez-Persem, *et al.*, Four core properties of the human brain valuation system demonstrated in intracranial signals. *Nat. Neurosci.* **23**, 664–675 (2020).

39. R. Abitbol, *et al.*, Neural Mechanisms Underlying Contextual Dependency of Subjective Values: Converging Evidence from Monkeys and Humans. *J. Neurosci.* **35**, 2308–2320 (2015).

40. C. Padoa-Schioppa, Neuronal origins of choice variability in economic decisions. *Neuron* **80**, 1322–1336 (2013).

41. V. Kurtz-David, D. Persitz, R. Webb, D. J. Levy, D. J. L. Room, "The Neural Computation of Inconsistent Choice Behavior" (February 22, 2019).

42. R. Webb, I. Levy, S. C. Lazzaro, R. B. Rutledge, P. W. Glimcher, Neural random utility: Relating cardinal neural observables to stochastic choice behavior. *J. Neurosci. Psychol. Econ.* **12**, 45–72 (2019).

43. S. J. Moeller, R. Z. Goldstein, Impaired self-awareness in human addiction : deficient attribution of personal relevance. *Trends Cogn. Sci.* **18**, 635–641 (2014).

44. J. Sui, X. Gu, Self as Object: Emerging Trends in Self Research. *Trends Neurosci.* **40**, 643–653 (2017).

45. G. Sescousse, X. Caldú, B. Segura, J. C. Dreher, Processing of primary and secondary rewards: A quantitative meta-analysis and review of human functional neuroimaging studies. *Neurosci. Biobehav. Rev.* **37**, 681–696 (2013).

46. V. S. Chib, A. Rangel, S. Shimojo, J. P. O'Doherty, Evidence for a Common Representation of Decision Values for Dissimilar Goods in Human Ventromedial Prefrontal Cortex. *J. Neurosci.* **29**, 12315–12320 (2009).

47. D. J. Levy, P. W. Glimcher, Comparing Apples and Oranges: Using Reward-Specific and Reward-General Subjective Value Representation in the Brain. *J. Neurosci.* **31**, 14693–14707 (2011).

48. D. McNamee, A. Rangel, J. P. O'Doherty, Category-dependent and category-independent goal-value codes in human ventromedial prefrontal cortex. *Nat. Neurosci.* **16**, 479–485 (2013).

49. R. Schandry, Heartbeat perception and emotional experience. *Psychophysiology* **18**, 483–488 (1981).

50. G. Zamariola, P. Maurage, O. Luminet, O. Corneille, Interoceptive accuracy scores from the heartbeat counting task are problematic: Evidence from simple bivariate correlations. *Biol. Psychol.* **137**, 12–17 (2018).

51. C. Ring, J. Brener, K. Knapp, J. Mailloux, Effects of heartbeat feedback on beliefs about heart rate and heartbeat counting: A cautionary tale about interoceptive awareness. *Biol. Psychol.* **104**, 193–198 (2015).

52. O. Desmedt, O. Luminet, O. Corneille, The heartbeat counting task largely involves non-interoceptive processes: Evidence from both the original and an adapted counting task. *Biol. Psychol.* **138**, 185–188 (2018).

53. A. Beck, C. H. Ward, M. Mendelson, J. Mock, J. Erbaught, An Inventory for Measuring Depression. *Arch. Gen. Psychiatry* **4**, 561–71 (1961).

54. E. Peters, S. Joseph, S. Day, P. Garety, Measuring Delusional Ideation: The 21-Item Peters et aL Delusions Inventory (PDI). *Schizophr. Bull.* **30**, 1005–1022 (2004).

55. C. D. Spielberger, R. L. Gorsuch, R. Lushene, P. R. Vagg, G. A. Jacobs, "Manual for the State-Trait Anxiety Inventory" in *Consulting Psychologists*, (1983).

56. E. B. Foa, *et al.*, The Obsessive-Compulsive Inventory: Development and validation of a short version. *Psychol. Assess.* **14**, 485–496 (2002).

57. M. A. Gray, *et al.*, A cortical potential reflecting cardiac function. *PNAS* **104**, 6818–6823 (2007).

58. W. G. Kubicek, R. P. Patterson, D. A. Witsoe, Impedance Cardiography As a Noninvasive Method of Monitoring Cardiac Function and Other Parameters of the Cardiovascular System. *Ann. N. Y. Acad. Sci.* **170**, 724–732 (1970).

59. A. Sherwood, *et al.*, Methodological Guidelines for Impedance Cardiography.

Psychophysiology **27**, 1–23 (1990).

60. G. G. Berntson, K. S. Quigley, D. Lozano, "Cardiovascular Psychophysiology" in *Handbook of Psychophysiology*, 3rd Ed., J. T. Cacioppo, L. G. Tassinary, G. Berntson, Eds. (Cambridge University Press, 2007), pp. 182–210.

61. A. Delorme, S. Makeig, EEGLAB: an open source toolbox for analysis of single-trial EEG dynamics including independent component analysis. *J. Neurosci. Methods* **134**, 9–21 (2004).

62. R. Oostenveld, P. Fries, E. Maris, J. M. Schoffelen, FieldTrip: Open source software for advanced analysis of MEG, EEG, and invasive electrophysiological data. *Comput. Intell. Neurosci.* **2011**, 1–9 (2011).

63. M. Vinck, M. van Wingerden, T. Womelsdorf, P. Fries, C. M. A. Pennartz, The pairwise phase consistency: A bias-free measure of rhythmic neuronal synchronization. *Neuroimage* **51**, 112–122 (2010).

64. G. Dirlich, L. Vogl, M. Plaschke, F. Strian, Cardiac field effects on the EEG. *Electroencephalogr. Clin. Neurophysiol.* **102**, 307–315 (1997).

65. R. E. Kass, A. E. Raftery, Bayes factors. *J. Am. Stat. Assoc.* **90**, 773–795 (1995).

66. F. Liang, R. Paulo, G. Molina, M. A. Clyde, J. O. Berger, Mixtures of g priors for Bayesian variable selection. *J. Am. Stat. Assoc.* **103**, 410–423 (2008).

67. B. Fischl, *et al.*, Automatically Parcellating the Human Cerebral Cortex. *Cereb. Cortex* **14**, 11–22 (2004).

68. F. Tadel, S. Baillet, J. C. Mosher, D. Pantazis, R. M. Leahy, Brainstorm: A user-friendly application for MEG/EEG analysis. *Comput. Intell. Neurosci.* **2011**, 879716 (2011).

69. N. Tzourio-Mazoyer, *et al.*, Automated anatomical labeling of activations in SPM using a macroscopic anatomical parcellation of the MNI MRI single-subject brain. *Neuroimage* **15**, 273–89 (2002).

70. F.-X. Neubert, R. B. Mars, J. Sallet, M. F. S. Rushworth, Connectivity reveals relationship of brain areas for reward-guided learning and decision making in human and monkey frontal cortex. *Proc. Natl. Acad. Sci. U. S. A.* **112**, E2695-704 (2015).

Author contributions

DA, SP and CTB designed the study. DA collected the data. DA, CTB and AB analyzed the data. DA and CTB interpreted the results and wrote the first draft of the paper. All authors contributed to the final version of the paper.

Competing interests

The authors declare no competing interests.

Data availability

The data that support the findings of this study are available from the corresponding authors upon reasonable request. Note that participants did not sign an explicit consent for public data sharing at the time of recordings.

Code availability

The custom code used for the main analyses of this paper can be accessed online at https://github.com/DamianoAzzalini/HER-preferences.